Chemical Physics Letters 701 (2018) 22–29

Contents lists available at ScienceDirect

Chemical Physics Letters

journal homepage: www.elsevier.com/locate/cplett

Research paper

Semi-flexible polymer engendered aggregation/dispersion of fullerene (C_{60}) nano-particles: An atomistic investigation

Sunil Kumar [a,*], Sudip K. Pattanayek [b]

[a] CSIR-National Metallurgical Laboratory, Jamshedpur 831007, India
[b] Indian Institute of Technology, New Delhi 110016, India

ARTICLE INFO

Article history:
Received 9 February 2018
In final form 16 April 2018
Available online 17 April 2018

Keywords:
Semi-flexible polymer
Fullerene
Molecular dynamics simulations
LAMMPS

ABSTRACT

Semi flexible polymer chain has been modeled by choosing various values of persistent length (stiffness). As the polymer chain stiffness increases, the shape of polymer chain changes from globule to extended cigar to toroid like structure during cooling from a high temperature. The aggregation of fullerene nano-particles is found to depend on the morphology of polymer chain. To maximize, the number of polymer bead-nanoparticle contacts, all nano-particle have positioned inside the polymer globule. To minimize, the energy penalty, due to bending of the polymer chain, all nano-particle have positioned on the surface of the polymer's cigar and toroid morphology.

1. Introduction

The addition of fullerene (C_{60}) nano-particle into polymer matrix have found to improve the mechanical [1,2], optical [3], thermal [4], electrical [5], barrier [6] properties. Dispersion and aggregation of fullerene nano-particles have been controlled most of the above mentioned properties of polymer nano-composite. Dispersion of nano-particles enhanced the interface area between the nano-particles and the polymer matrix, therefore polymer nano-composite show much better properties even at a low quantity of nano-particles. However, dispersion and aggregation of nano-particles will also depend on the various characteristics of polymer matrix such as semi-flexibility, polymer chain length, etc. Variation in semi-flexibility of polymer chains leads to lamellar (cigar like), toroid and globule morphology. These organizations of polymer chain segments significantly influence the distribution of nano-particles in a polymer matrix. Therefore, we have studied semi-flexible polymer chain induces aggregation/dispersion of nano-particle using molecular dynamics simulations.

Atomistic [7–17] and coarse grained (or united atom) [18–49] molecular dynamics simulations have been developed to study the various multi-scale characteristics of soft materials at various temperature, pressure and solvency conditions. Atomistic molecular dynamic simulation has been widely used for the investigations of various inter- and intra-atomic interactions between atoms of polymer [7–12], DNA [13], dendrimers [14–17] and its effect over the transformations between globules to extended structure. Benyamini et al. [54] has investigated various interactions between fullerene and various proteins using docking and binding site alignment using atomistic model. They found similarities between the (human and bovine) serum albumins and the HIV-protease binding sites, but the binding site of the fullerene-specific antibody has found to be different from the others.

In case of coarse grain (or united atom) [18–49] molecular dynamics simulations, group of atoms considered as a single bead or united atom, by freezing the quantum and atomic properties of the materials. United atom molecular dynamics simulations extensively used to investigate polymer crystallization in bulk [18–26] and in the vicinity of nano-fillers. Kavassalis and Sundararajan [18,19] demonstrated an unambiguous transition of globular to a folded crystalline structure of polymers using united atom molecular dynamics simulations. They considered a single polyethylene chain in a vacuum, where all possible effects of solvent molecules were ignored. In addition, they have considered much stiffer polyethylene chain than real polyethylene, and they have shown that the crystallization rate is sensitive to the chain stiffness. Muthukumar et al. [23] has shown that the long polymer chain first formed local crystalline regions as "baby nuclei", which then gradually coalesced and formed a large chain folded crystal by united atom model. They have studied primary nucleation and growth of crystallites at the fixed polymer chain stiffness.

Entanglement effect, comparative size effect, inters and intra-atomic interactions over the aggregation/dispersion of nano-particle in polymer matrix have been studied by united atom molecular dynamics simulations extensively [27–39]. Yang et al.

* Corresponding author.
E-mail address: sunil@nmlindia.org (S. Kumar).

https://doi.org/10.1016/j.cplett.2018.04.035
0009-2614/

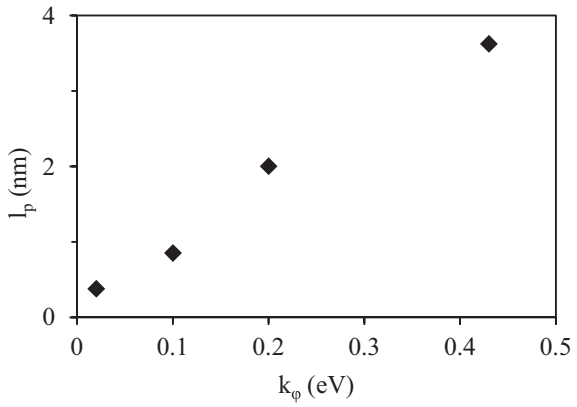

Fig. 1. Variation of persistence length of polymer chain with k_φ at 300 K.

[27] have shown the isothermal crystallization process of polyethylene/C_{60} nano-composites using united atom model of molecular dynamics simulation method. They have found that the fullerene molecules are excluded from the crystal region of the polyethylene/C_{60} nano-composites. Vogiatzis and Theodorou [8] have used both atomistic and coarse grained models to investigate the segmental dynamics of polystyrene in the presence of fullerene (C_{60}) nano-particles. They have found that the inclusion of fullerene nano-particles reduces the segmental dynamics of polystyrene. Most of the investigations concerned with the effect of polymer-fullerene interaction and polymer-polymer interaction, but they have not studied the effect of polymer chain stiffness over the aggregation and dispersion of nano-particles.

In the present study, we have employed united atom model for molecular dynamics simulations to find out long semi-flexible polymer chain engendered aggregation/dispersion of nano-particles. The practical applications of present system (a semi-

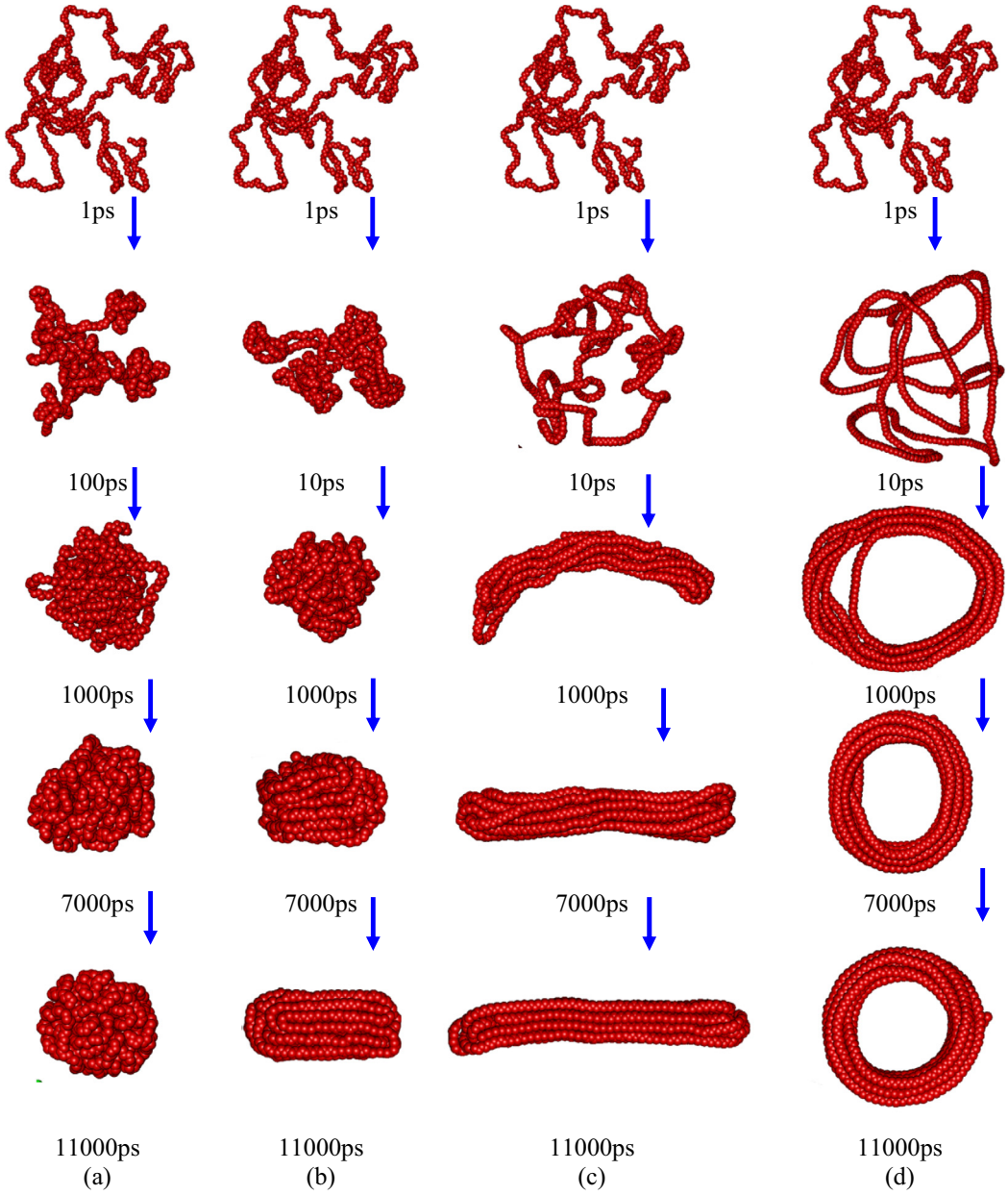

Fig. 2. The evolution of various structures of polymer chain as the simulation time increases during step-wise cooling from 800 K to 300 K: (a) k_φ = 0.02, (b) k_φ = 0.2, (c) k_φ = 0.5 and (d) k_φ = 2 eV.

flexible polymer chain and a few nano-particles) are in understanding the condensation of Deoxyribonucleic acid (DNA) using cationic dendrimers, which has application in gene therapy [40] and use of fullerene derivatives mediated inhibition of HIV-1 Replication [55]. We note that stiffness of semi-flexible polymer depends on the environment of the protein or DNA. Thus, stiffness parameter can mimic the condition of the environment. Using molecular dynamics simulations, Lappala and Terentjev [41] have shown that the globule to the extended toroid transition of a long single semi flexible polymer chain can mimic tapping-mode AFM height topo grams of xanthan–chitosan compaction at room temperature. Our results may be useful to understand the activity of polymer and bio-polymer to construct novel materials in nanotechnologies.

2. Simulation method

Molecular Dynamics (MD) simulation [42,43] has been used for aggregation and dispersion of fullerene nano-particle in the presence of semi-flexible polymer. A semi-flexible polymer chain consists of N_b number of beads. Each bead of a semi-flexible polymer chain can interact via bonded, angle, torsion and non-bonded interaction potential as described in the supporting information. The general equation of motion of i^{th} bead during molecular dynamic simulation is given by

$$m\frac{\partial^2 \mathbf{r}_i}{\partial t^2} = -\nabla E_i - \frac{m}{\zeta}\frac{\partial \boldsymbol{r}_i}{\partial t} + \boldsymbol{\xi}_i(t) \quad (1)$$

where the total energy of i^{th} bead is denoted by E_i. $\boldsymbol{r}_i$ is the position of the i^{th} bead in the simulation box; t is time; $\frac{m}{\zeta} = \Gamma$is a friction coefficient between beads, $\zeta$is the damping constant, and $\boldsymbol{\xi}_i(t)$ describes the random force acting on the i^{th} bead. The Nose–Hoover thermostat [44,45] was implemented to control the desired temperature of the system along with the velocity-Verlet algorith m [46] with a time step of 1 fs. The simulation temperature was decreased from 800 K to 300 K in the steps of 50 K. Simulations were run for 1000 ps at each temperature step during cooling as reported in our previous studies [47,48]. The values of all parameters for polymer nano-particle system were based on the DREIDING [49] force field. In a few simulations, we varied k_φ to see the effect of chain flexibility on its organization. Molecular dynamics simulations, visualizations, and analysis of polymer fullerene nano-composite systems were carried out by Large-scale Atomic/Molecular Massively Parallel Simulator (LAMMPS) [50], Visual Molecular Dynamics (VMD) [51], Open Visualization Tool (OVITO) [52], and DL_POLY [53], software packages, respectively.

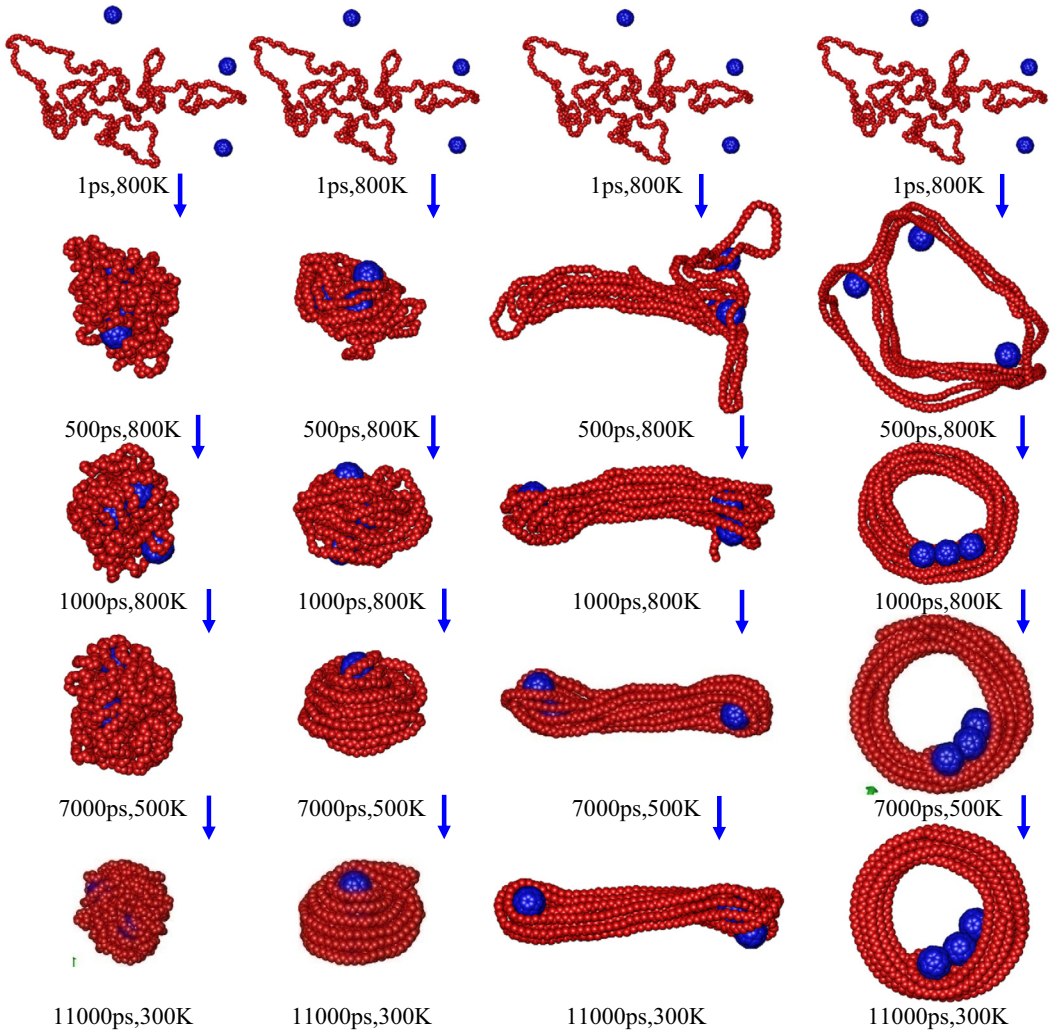

Fig. 3. The evolution of various structures of polymer/C_{60} composite as the simulation time increases during step-wise cooling from 800 K to 300 K: (a) k_φ = 0.02, (b) k_φ = 0.2, (c) k_φ = 0.5 and (d) k_φ = 2 eV.

Semi-flexibility of a polymer can be realized by its persistence length, which can be obtained from theoretically and experimental data. We have determined the persistence length by the projection of all the bond vectors along the first bond vector of a polymer chain. Thus, the persistence length can be related to the torsional bending constant, k_φ of a polymer chain at a very high value of k_φ. To make a correlation between persistence length and k_φ, we equilibrate a polymer chain of 100 beads at 300 K. The persistence length of a polymer chain is calculated as given by the relation:

$$\langle \hat{b}(s) \cdot \hat{b}(0) \rangle = exp\left(-\frac{s}{l_P}\right) \quad (2)$$

where l_P is the persistence length of polymer, $\hat{b}(s)$ is the sub-bond vector $b_i = \frac{1}{2}(l_i + l_{i+1})$, l_i is the bond vector at a distance s along the path of the chain. The calculated value of persistent length of a polymer chain at various values of torsion angle potential constant k_φ is plotted in Fig. 1.

The persistence length of chains with k_φ = 0.02, 0.1 and 0.2 eV are 0.37, 0.85 and 1.96 nm respectively.

3. Results

We have taken a system containing a polymer chain consists of 1000 beads in a simulation box. Fig. 2 shows the snapshots of polymers of four different k_φ values, lowest values (k_φ = 0.02 eV) and highest values (k_φ = 2 eV), representing flexible and stiff polymer chain respectively. The moderate semi-flexibility of polymer chain are categorized in two parts, first is low to moderate value (such as k_φ = 0.02–0.2 eV) and moderate to high value (such as k_φ = 0.2–1 eV). Four distinct final conformations are found during cooling from 800 K to 300 K depending on the k_φ. These are spherical globules, elongated globule, cigar and toroid like structure. The four columns of Fig. 2, shows the snapshot of polymer chain of four stiffness values belongs each category, such as lowest (k_φ = 0.02 eV), low to moderate value (k_φ = 0.2 eV), moderate to high value (k_φ = 0.5 eV) and highest values (k_φ = 2 eV). The flexible polymer chain (low values k_φ = 0.02 eV) shows the spherical collapse structure as system temperature cooling from 800 K to 300 K. At a high temperature, polymer chain segments are in coil or swollen state and as system temperature decreases, chain segments are starting to aggregate. Finally, at 300 K, polymer chain segments make a spherical globular structure as shown in Fig. 2(a). The organization of polymer chain segments found random or non-periodic pattern due to the flexible nature of polymer chain. In case of low stiffness (k_φ = 0.2 eV), polymer chain segments make a short length lamellar organization as system temperature cooled from 800 K to 300 K, which looks like a cigar. The evolution of a cigar like structure found through randomly aggregation of chain segments in globular shape and as the simulation proceeds randomly organization convert into the lamella organization as shown in Fig. 2(b). In case of moderate stiffness (k_φ = 0.5 eV), polymer chain segments make a long lamellar organization, which also looks like a cigar. The evolution of long cigar like structure found directly lamellar aggregation of chain segments initial swollen state during the simulation as shown in Fig. 2(c). In case of high stiffness (k_φ = 2 eV), polymer chain segments make a circular organization, which looks like a toroid as shown in Fig. 2(d).

Fig. 3 shows the snapshot of aggregation and organization process of polymer and C_{60} nano-particle as simulation proceeds and system temperature cooled down from 800 K to 300 K. The snap-

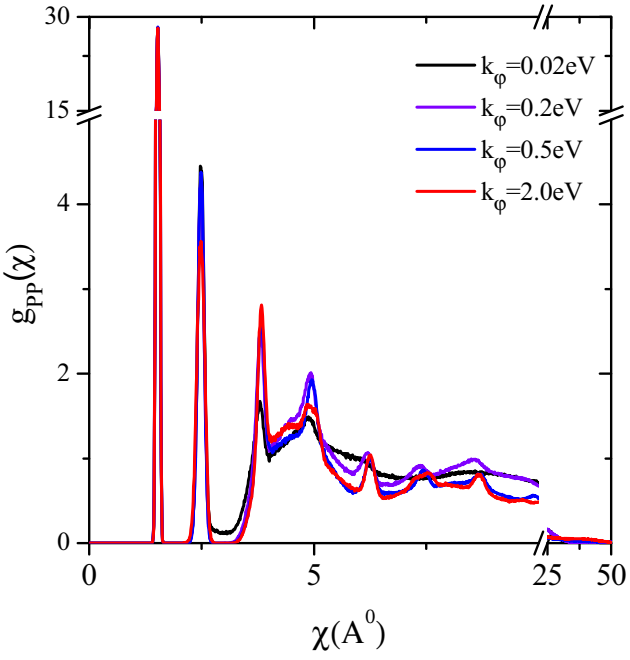

Fig. 5. Radial distribution functions $g_{PP}(\chi)$ of various polymer/nano-particle structures at equilibrium.

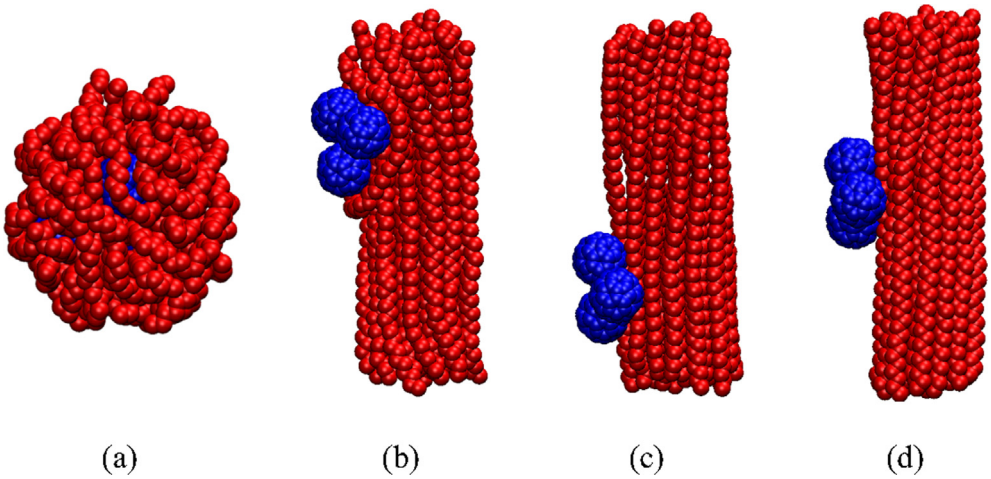

Fig. 4. Snapshot of polymer/C_{60} composite system, consists of 3 fullerene nano-particle and 20 polymer chains (50 beads per chain): (a) k_φ = 0.02, (b) k_φ = 0.2, (c) k_φ = 0.5 and (d) k_φ = 2 eV.

shot shows that the aggregation and organization behaviour significantly depends on the stiffness parameters (k_φ) of polymer chain as discussed earlier. We have considered a wide range of different values of polymer chain stiffness such as k_φ = 0.02–2 eV. These snapshots show that the C_{60} cannot stay within the organized/aligned region of the polymer and they should be located outside the crystal regions. The C_{60} has a large curved surface, which does not fit the lamellar organization of polymer chain. Thus, the C_{60} molecules cannot induce the polymer organization and are excluded from the organized/aligned region of the polymer/C_{60} nano-composites. Fig. 4(a)–(d) depict the aggregation of fullerene nano-particles in the multi chain systems at various values of k_φ. At k_φ = 0.02 eV, polymer chains depict globular structure and all fullerene nano-particles located inside the globule. However, as value of k_φ increases, polymer shows cigar like structure and all fullerene nano-particles located over the cigar.

The radial distribution functions $g_{PP}(\chi)$ of polymer chain segments in the presence spherical nano-particles are shown in Fig. 5. The region 0 < χ < 3.634 Å is dominated by the bonded (i^{th} and i + 1th) and bond angled (i^{th} and i + 2th) polymer beads. In this region, $g_{PP}(\chi)$ vs χ plot shows two sharp and long peak corresponds to bonded and bond angled polymer beads and it is a nearly independent of aggregation or organization inter-segments of polymer chain. The region 3.634 < χ < 5.54 Å is showing the addition of both intra and inter segmental polymer beads. The moderately broad and high peaks at 3.8 Å and 4.8 Å are representing the combined contribution of both short rang ordered in an intra-segment and aggregation of inter-segmental beads of polymer chain. Above χ = 5.54 Å, $g_{PP}(\chi)$ vs χ plot shows the significant contribution of long range ordered organization and aggregation of both intra and inter-segmental beads. The trans conformation in intra-segments show many short peak at regular interval as going

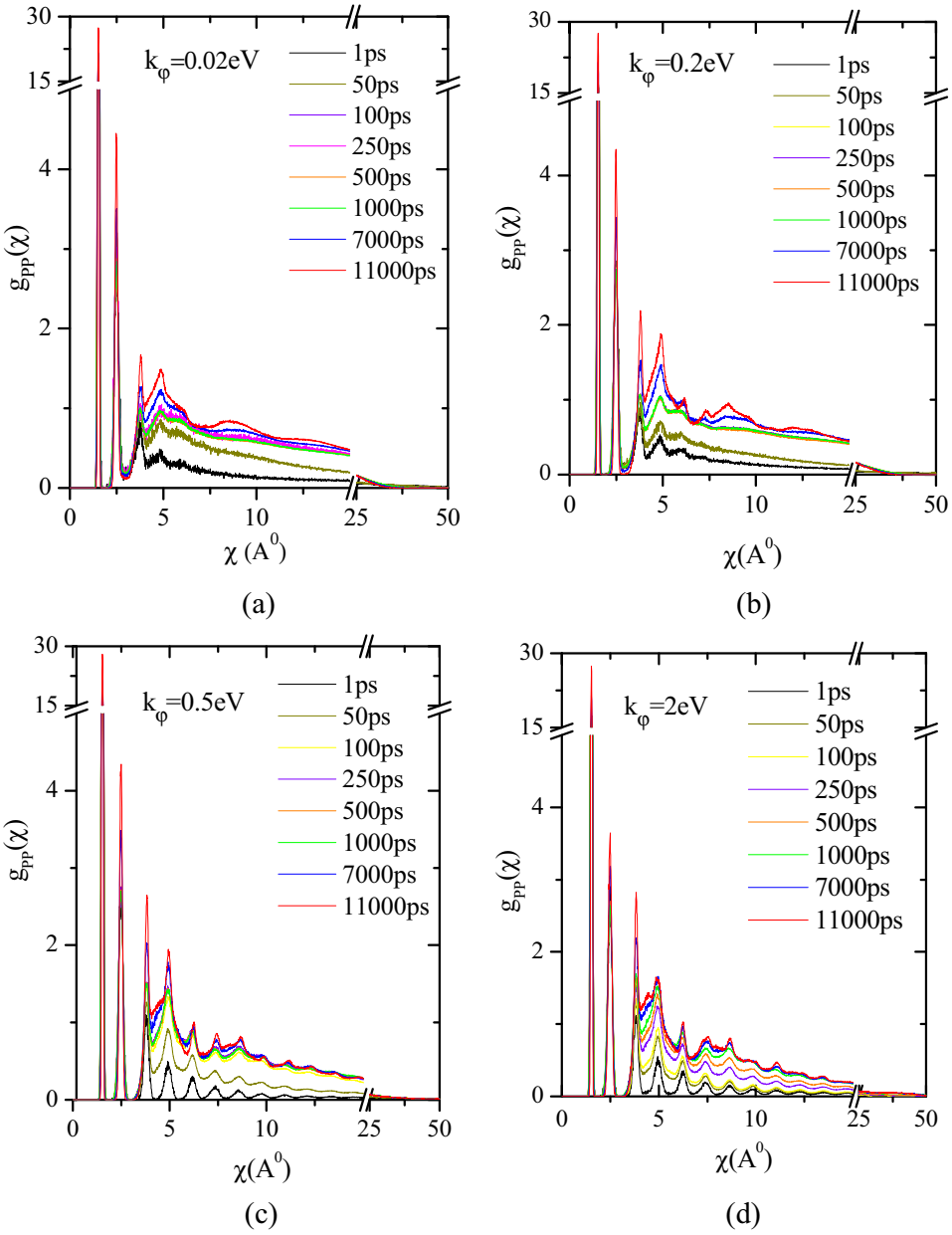

Fig. 6. Radial distribution function $g_{PP}(\chi)$ of polymer chain structure formation in presence of nano-particle at various times during stepwise cooling from 800 K to 300 K: (a) k_φ = 0.02, (b) k_φ = 0.2, (c) k_φ = 0.5 and (d) k_φ = 2 eV.

above $\chi \geq 5.54$ Å. The collapse state ($k_\varphi = 0.02$ eV), $g_{PP}(\chi)$ vs χ plot does not show any distinguishable peaks after $\chi \geq 5.54$ Å due to random packing of polymer chain segments. For other structure, polymer chain segments packed into ordered organization which is identified through many small peaks of $g_{PP}(\chi)$ after $\chi \geq 5.54$ Å. This is also indicating that polymer chain segments are more regularly packed and separations between beads in intra-segments are uniform.

We have plotted the time evolution of radial distribution function $g(\chi)$ for different values k_φ in Fig. 6. At a low value of polymer chain stiffness (such as $k_\varphi = 0.02$ eV), the final collapse structure evolves through aggregate formation. The aggregation is indicated by the appearance of a peak at $\chi = 4.87$ Å and subsequent plateau value of $g(\chi)$ at $\chi > 5.54$ Å. At the next higher value of $k_\varphi = 0.2$ eV, $g(\chi)$ vs χ plot suggests that initially (time < 7000 ps), the polymer forms aggregates and subsequently arrange into regular packing (peaks appear at $\chi \geq 6.28$ Å). We note that the polymer before crystallization may proceed through the collapse structure formation. The plot of $g(\chi)$ vs χ for $k_\varphi = 0.5$ eV suggests that the polymer beads arrange regularly to form the final structure. Comparatively, the $g(\chi)$ vs χ plots for polymers with $k_\varphi = 0.2$ and 0.5 eV, we can state that the final morphology of the polymers is similar, but the evolutionary process is different. The radial distribution functions $g_{NP}(\chi)$ for polymer chain segments packing around the C_{60} is shown in Fig. 7. The first peak $g_{NP}(\chi)$ is found nearly in the region of $3.5 < \chi < 5.5$ Å, which is just above the bead diameter (3.898 Å) of C_{60} nano-particle. The exact position of peaks depends on the polymer chain stiffness.

Fig. 8 shows the evolution of bond order parameter for various polymer structures for both absence and presence of C_{60} nano-particle. For collapse state ($k_\varphi = 0.02$ eV), the bond order parameter found very less and near to zero due to random organization of polymer chain. For $k_\varphi = 0.2$ eV, the following steps are found in organizations: At a high temperature above T = 550 K (below 6000 ps), the parameter S fluctuates at a low value (≈0.1), which shows that there is no ordered organization between polymer segments in this temperature region. At a temperature lower than T < 550 K (above 6000 ps), S gradually increases as the temperature decreases, which indicates that the polymer chain starts to grow in ordered organizations. At a temperature lower than T < 350 K, the growth rate of the orientation order becomes small. The reason for this is that, in this temperature region, the global conformational change of the polymer chain ceases and only the local motion of united atoms with no global change takes place. For $k_\varphi = 0.5$ (long cigar) and $k_\varphi = 2$ (toroid like structure), the bond order parameter increases at a very early stage of the simulation. We have compared the bond order of pure polymer (in the absence of nano-particle) and polymer with C_{60}. Pure polymer shows

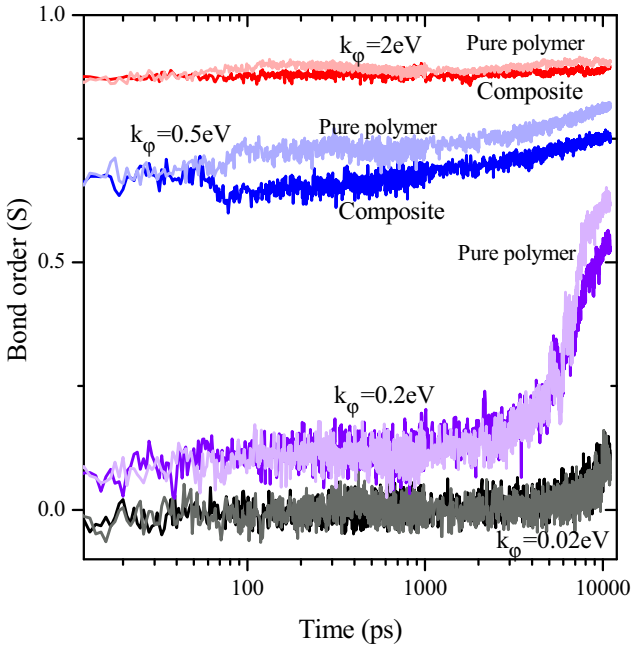

Fig. 8. Comparison of bond order parameter (S) of polymer and polymer nano-particle composite for various values of k_φ.

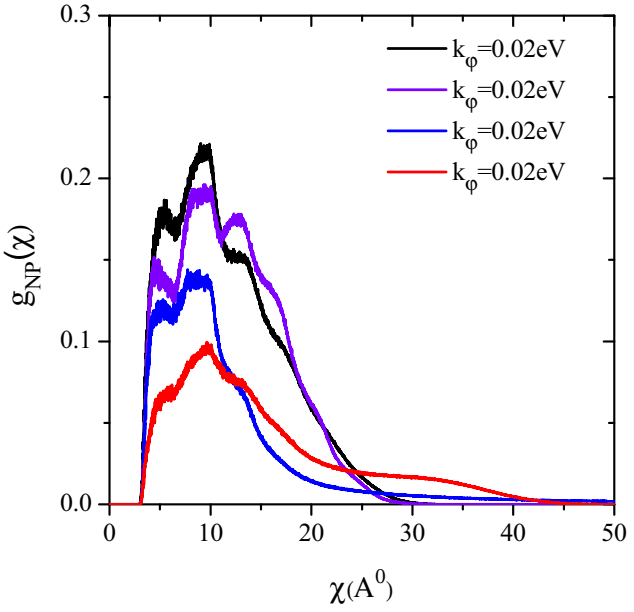

Fig. 7. Radial distribution functions $g_{NP}(\chi)$ of various polymer/C_{60} structures at equilibrium.

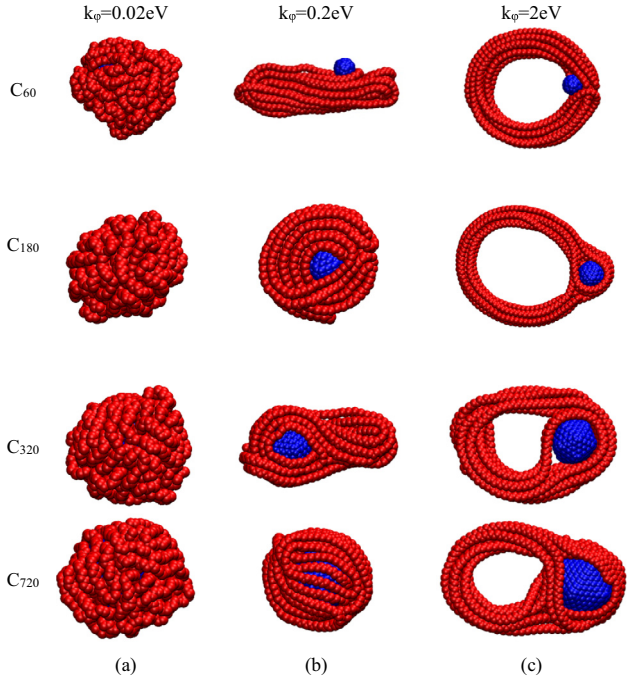

Fig. 9. Effect of nano-particle (bucky-balls) size over the polymer chain organization: (a) $k_\varphi = 0.02$ eV, (b) $k_\varphi = 0.2$ eV and (c) $k_\varphi = 2$ eV.

higher bond order parameter in all types of structure except collapse structure. Two major reasons for lesser bond order parameter in polymer/C_{60} composite are as follows. (a) The inclusion of C_{60}, restricts the motion of polymer chain segments due to non-bonded interaction between the polymer and C_{60} beads. (b) A large curved surface C_{60} does not fit with the lamellar organization of polymer chain.

Fig. 9 depicts polymer chain organizations in the vicinity of nano-particle (bucky-ball) of different sizes such as C_{60}, C_{180}, C_{320} and C_{720}. In case of k_φ = 0.2 eV, polymer chain segments organized randomly over the nano-particles as shown in Fig. 9(a). However, as the value of k_φ increases, polymer chain segments organizes into cigar and toroid like structures and subsequently, nano-particles come out from the polymer segments as shown in Fig. 9(b) and (c). These snapshots show that the tiny nano-particles cannot stay within the organized/aligned region of the polymer. However, comparatively bigger nano-particles facilitate the semi-flexible polymer chain wrapped around them. From these simulations, it has been found that polymer stiffness, polymer chain length and nano-particle size is the major factors to control the overall properties of polymer nano-composite.

4. Conclusions

The molecular dynamics simulations study provides new insight on the organization of single polymer in presence/absence of C_{60} nano-particles. The organization of polymer depends on chain stiffness. As polymer chain stiffness increases, the shape of polymer structure at equilibrium change from spherical to extended cigar to toroid. A location of C60 nano-particle inside/outside depends on the polymer chain's organization. In case of a random organization, all nano-particle has positioned inside the polymer structure. But in cigar and toroid like structure, all nano-particle have located on the surface of the polymer. In the presence of nano-particles, bond-order parameters of the polymer chain decrease due to a very small size of nano-particle compared to the polymer. The small size of C_{60}, does not facilitate polymer nucleation but non-bonded interactions between polymer and C_{60} restricts the motion of polymer chain segments.

References

[1] M.S. Dresselhaus, G. Dresselhaus, P.C. Eklund, Science of Fullerenes and Carbon Nanotubes: Their Properties and Applications, Elsevier, 1996.
[2] F.L. De La Puente, J.F. Nierengarten, Fullerenes: Principles and Applications, Royal Society of Chemistry, 2011.
[3] T. Erb, U. Zhokhavets, G. Gobsch, S. Raleva, B. Stühn, P. Schilinsky, C. Waldauf, C.J. Brabec, Correlation between structural and optical properties of composite polymer/fullerene films for organic solar cells, Adv. Funct. Mater. 15 (2005) 1193–1196.
[4] N.C. Cates, R. Gysel, Z. Beiley, C.E. Miller, M.F. Toney, M. Heeney, I. McCulloch, M.D. McGehee, Tuning the properties of polymer bulk heterojunction solar cells by adjusting fullerene size to control intercalation, Nano Lett. 9 (2009) 4153–4157.
[5] I. Riedel, J. Parisi, V. Dyakonov, L. Lutsen, D. Vanderzande, J.C. Hummelen, Effect of temperature and illumination on the electrical characteristics of polymer-fullerene bulk-heterojunction solar cells, Adv. Funct. Mater. 14 (2004) 38–44.
[6] R.A. Khan, D. Dussault, S. Salmieri, A. Safrany, M. Lacroix, Mechanical and barrier properties of carbon nanotube reinforced PCL-based composite films: effect of gamma radiation, J. Appl. Polym. Sci. 127 (2013) 3962–3969.
[7] P.A. Olsson, E. Schröder, P. Hyldgaard, M. Kroon, E. Andreasson, E. Bergvall, Ab initio and classical atomistic modelling of structure and defects in crystalline orthorhombic polyethylene: twin boundaries, slip interfaces, and nature of barriers, Polymer 121 (2017) 234–246.
[8] G.G. Vogiatzis, D.N. Theodorou, Local segmental dynamics and stresses in polystyrene–C_{60} mixtures, Macromolecules 47 (2013) 387–404.
[9] C.T. Lu, A. Weerasinghe, D. Maroudas, A. Ramasubramaniam, A comparison of the elastic properties of graphene-and fullerene-reinforced polymer composites: the role of filler morphology and size, Sci. Rep. 6 (2016) 31735.
[10] R. Rafiee, M. Mahdavi, Characterizing nanotube–polymer interaction using molecular dynamics simulation, Comput. Mater. Sci. 112 (2016) 356–363.
[11] V.M. Nazarychev, A.V. Lyulin, S.V. Larin, A.A. Gurtovenko, J.M. Kenny, S.V. Lyulin, Molecular dynamics simulations of uniaxial deformation of thermoplastic polyimides, Soft Matter 12 (2016) 972–3981.
[12] W. Wang, Y. Tanaka, T. Takada, S. Iwata, H. Uehara, S. Li, Influence of oxidation on the dynamics in amorphous ethylene-propylene-diene-monomer copolymer: a molecular dynamics simulation, Polym. Degrad. Stab. 147 (2018) 187–196.
[13] G.M. Pavan, M.A. Mintzer, E.E. Simanek, O.M. Merkel, T. Kissel, A. Danani, Computational insights into the interactions between DNA and siRNA with "rigid" and "flexible" triazine dendrimers, Biomacromolecules 11 (2013) 721–730.
[14] V. Vasumathi, P.K. Maiti, Complexation of siRNA with dendrimer: a molecular modeling approach, Macromolecules 43 (2010) 8264–8274.
[15] B. Nandy, P.K. Maiti, DNA compaction by a dendrimer, J. Phys. Chem. B 115 (2010) 217–230.
[16] T. Mandal, C. Dasgupta, P.K. Maiti, Engineering gold nanoparticle interaction by PAMAM dendrimer, J. Phys. Chem. C 117 (2013) 13627–13636.
[17] S. Riniker, J.R. Allison, W.F. van Gunsteren, On developing coarse-grained models for biomolecular simulation: a review, PCCP 14 (2012) 12423–12430.
[18] T.A. Kavassalis, P.R. Sundararajan, A molecular-dynamics study of polyethylene crystallization, Macromolecules 26 (1993) 4144–4150.
[19] P.R. Sundararajan, T.A. Kavassalis, Molecular dynamics study of polyethylene chain folding: the effects of chain length and the torsional barrier, J. Chem. Soc., Faraday Trans. 91 (1995) 2541–2549.
[20] A. Lappala, E.M. Terentjev, "Raindrop" coalescence of polymer chains during coil-globule transition, Macromolecules 46 (2013) 1239–1247.
[21] L. Larini, D. Leporini, A manifestation of the Ostwald step rule: molecular-dynamics simulations and free-energy landscape of the primary nucleation and melting of single-molecule polyethylene in dilute solution, J. Chem. Phys. 123 (2005) 144907.
[22] G. Maurstad, B.T. Stokke, Toroids of stiff polyelectrolytes, Curr. Opin. Colloid Interface Sci. 10 (2005) 16–21.
[23] M. Muthukumar, P. Welch, Modeling polymer crystallization from solutions, Polymer 41 (2000) 8833–8837.
[24] P. Anjukandi, G.G. Pereira, M.A.K. Williams, Langevin dynamics simulations reveal biologically relevant folds arising from the incorporation of a torsional potential, J. Theor. Bio. 265 (2010) 245–249.
[25] Y. Takenaka, K. Yoshikawa, Y. Yoshikawa, Y. Koyama, T. Kanbe, Morphological variation in a toroid generated from polymer chain, J. Chem. Phys. 123 (2005) 014902.
[26] M.-X. Wang, Effect of coil-globule transition on the single-chain crystallization, J. Phys. Chem. B 117 (2013) 6541–6546.
[27] H. Yang, X.J. Zhao, Z.Y. Lu, F.D. Yan, Temperature influence on the crystallization of polyethylene/fullerene nanocomposites: molecular dynamics simulation, J. Chem. Phys. 131 (2009) 234906.
[28] D. Brown, V. Marcadon, P. Mele, N.D. Alberola, Effect of filler particle size on the properties of model nanocomposites, Macromolecules 41 (2008) 1499–1511.
[29] D. Meng, S.K. Kumar, S. Cheng, G.S. Grest, Simulating the miscibility of nanoparticles and polymer melts, Soft Matter 9 (2013) 5417–5427.
[30] J. Cho, C.T. Sun, A molecular dynamics simulation study of inclusion size effect on polymeric nanocomposites, Comput. Mater. Sci. 41 (2007) 54–62.
[31] A.N. Enyashin, P.Y. Glazyrina, On the crystallization of polymer composites with inorganic fullerene-like particles, PCCP 14 (2012) 7104–7111.
[32] Y. Feng, H. Zou, M. Tian, L. Zhang, J. Mi, Relationship between dispersion and conductivity of polymer nanocomposites: a molecular dynamics study, J. Phys. Chem. B 116 (2012) 13081–13088.
[33] G. Gyanwali, R.S.H. Koralege, M. Hodge, K.D. Ausman, J.L. White, C60–polymer nanocomposite networks enabled by guest-host properties, Macromolecules 46 (2013) 6118–6123.
[34] Y. Li, M. Kröger, W.K. Liu, Nanoparticle geometrical effect on structure, dynamics and anisotropic viscosity of polyethylene nanocomposites, Macromolecules 45 (2012) 2099–2112.
[35] T.K. Patra, J.K. Singh, Coarse-grain molecular dynamics simulations of nanoparticle-polymer melt: dispersion vs. agglomeration, J. Chem. Phys. 138 (2013) 144901.
[36] R.A. Riggleman, G. Toepperwein, G.J. Papakonstantopoulos, J.-L. Barrat, J.J. de Pablo, Entanglement network in nanoparticle reinforced polymers, J. Chem. Phys. 130 (2009) 244903.
[37] Y. Termonia, Monte-Carlo modeling of dense polymer melts near nanoparticles, Polymer 50 (2009) 1062–1066.
[38] D. Zhang, H. Meyer, Molecular dynamics study of polymer crystallization in the presence of a particle, J. Polym. Sci., Part B: Polym. Phys. 45 (2007) 2161–2166.
[39] X. Zhao, A. Striolo, Peter T. Cummings, C60 binds to and deforms nucleotides, Biophys. J. 89 (2005) 3856–3862.
[40] M.L. Ainalem, T. Nylander, DNA condensation using cationic dendrimers—morphology and supramolecular structure of formed aggregates, Soft Matter 7 (2011) 4577–4594.
[41] A. Lappala, E.M. Terentjev, Maximum compaction density of folded semiflexible polymers, Macromolecules 46 (2013) 7125–7131.
[42] D.C. Rapaport, The Art of Molecular Dynamics Simulation, Cambridge University Press, 2004.
[43] M.P. Allen, D.J. Tildesley, Computer Simulation of Liquids, Oxford University Press, 2017.

[44] G.J. Martyna, D.J. Tobias, M.L. Klein, Constant pressure molecular dynamics algorithms, J. Chem. Phys. 101 (1994) 4177–4189.
[45] M. Parrinello, A. Rahman, Polymorphic transitions in single crystals: a new molecular dynamics method, J. Appl. Phys. 52 (1981) 7182–7190.
[46] L. Verlet, Computer "experiments" on classical fluids. I. Thermodynamical properties of Lennard-Jones molecules, Phys. Rev. 159 (1967) 98.
[47] S. Kumar, S.K. Pattanayek, G.G. Pereira, Organization of polymer chains onto long, single-wall carbon nano-tubes: effect of tube diameter and cooling method, J. Chem. Phys. 140 (2014) 024904.
[48] S. Kumar, S.K. Pattanayek, G.G. Pereira, Polymers encapsulated in short single wall carbon nanotubes: Pseudo-1D morphologies and induced chirality, J. Chem. Phys. 142 (2015) 114901.
[49] S.L. Mayo, B.D. Olafson, W.A. Goddard, DREIDING: a generic force field for molecular simulations, J. Phys. Chem. 94 (1990) 8897–8909.
[50] S. Plimpton, Fast parallel algorithms for short-range molecular dynamics, J. Comput. Phys. 117 (1995) 1–19.
[51] W. Humphrey, A. Dalke, K. Schulten, VMD: visual molecular dynamics, J. Mol. Graph. 14 (1996) 33–38.
[52] A. Stukowski, Visualization and analysis of atomistic simulation data with OVITO–the open visualization tool, Model. Simul. Mater. Sci. Eng. 18 (2009) 015012.
[53] I.T. Todorov, W. Smith, K. Trachenko, M.T. Dove, DL_POLY_3: new dimensions in molecular dynamics simulations via massive parallelism, J. Mater. Chem. 16 (2006) 1911–1918.
[54] H. Benyamini, A. Shulman-Peleg, H.J. Wolfson, B. Belgorodsky, L. Fadeev, M. Gozin, Interaction of C60-fullerene and carboxyfullerene with proteins: docking and binding site alignment, Bioconjugate Chemistry 17 (2006) 378–386.
[55] Z.S. Martinez, E. Castro, C.S. Seong, M.R. Cerón, L. Echegoyen, M. Llano, Fullerene derivatives strongly inhibit HIV-1 replication by affecting virus maturation without impairing protease activity, Antimicrob. Agents Chemother. 60 (2016) 5731–5741.